Polyhedra as $\pm J$ closed Ising lattices

J.F. Valdés, J. Cartes, and E.E. Vogel
Universidad de La Frontera, Departamento de Ciencias Físicas
Casilla 54-D, Temuco, Chile
e-mail: [1]*evogel@ufro.cl*

Recibido el 10 de noviembre de 1999; aceptado el 27 de marzo de 2000

Ising lattices are defined for regular polyhedra with spin occupying vertices and interactions laying along edges. Mixed ferromagnetic and antiferromagnetic interactions are considered, x being the concentration of the former. Competition among local fields brings in frustration making non trivial to solve for physical properties of such lattices. Here, we characterize the most important ground state properties of these systems such as energy, remanent entropy, average frustration segment, diluted lattice (including unfrustrated domains), and site order parameter. The functional dependence on x is established in each case, comparing among the 6 different polyhedra studied here. The rôle plaid by topology through aspects such as shape of faces and coordination number is brought out. When possible, a comparison with similar two-dimensional flat lattices is performed.

Keywords: Ising models; frustration; regular polyhedra

Se definen redes de Ising para poliedros regulares con espines ocupando los vértices e interacciones a lo largo de las aristas. Se consideran interacciones mixtas ferromagnéticas y antiferromagnéticas, siendo x la concentración de la primera. La competencia entre campos locales genera frustración haciendo no trivial la solución de las propiedades físicas de tales redes. Caracterizaremos las propiedades más importantes asociadas al nivel fundamental de estos sistemas, tales como energía, entropía remanente, segmento de frustración promedio, red diluida (incluyendo dominios sin frustración) y parámetro de orden de sitio. En cada caso se establece la dependencia funcional respecto de x, comparando entre los 6 poliedros estudiados aquí. Se establece el rol jugado por la topología mediante aspectos tales como forma de las caras y número de coordinación. En tanto es posible, se efectúa una comparación con redes planas bidimensionales similares.

Descriptores: Modelos de Ising; frustración; poliedros regulares

PACS: 75.10.Hk; 75.40.Mg; 75.50.Lk

1. Introduction

Ising lattices with mixed ferromagnetic ($-J$) and antiferromagnetic ($+J$) interactions have been studied for two decades as simple theoretical models for spin glasses [1, 2]. All of the abundant literature produced for this system and its variations needs to make assumptions for boundary conditions to keep uniform the coordination number through the system.

In the case of flat two-dimensional lattices, periodic boundary conditions are normally imposed. However, polyhedra are closed two-dimensional objects where no assumption needs to be made about boundary conditions. Our main interest here is to characterize ground state properties of closed $\pm J$ Ising lattices whose spins occupy the vertices, while interactions lay along the edges of regular polyhedra. Another interesting feature of polyhedra is that coordination number 5 can be studied besides 3, 4, and 6 that arise naturally in flat two dimensional Bravais lattices.

Previous work on two dimensional $\pm J$ Ising lattices has dealt with flat lattices with equal amount of ferromagnetic (F) and antiferromagnetic (AF) interactions [3]. In the present paper we want to make progress in two directions: a) calculating two dimensional lattices without need of defining specific boundary conditions, and b) varying x, the concentration of F interactions in the full range $[0, 1]$. Beyond previously reported properties for $x = 0.5$, such as ground-state energy per interaction, remanent entropy, average frustration segment and site order parameter, we would like to add here the new concept of diluted lattice [4] and its associated properties.

We concentrate here on the ground state properties of the following special two-dimensional objects: tetrahedron (S^4), octahedron (S^6), cube (S^8), icosahedron (S^{12}), and dodecahedron (S^{20}). We will also include the spherical Fullerene (S^{60}), which is very close to a regular polyhedron. The main characteristics of these geometrical artifacts are presented in Fig. 1.

These systems relate geometry and topology in different ways, so different properties show particular dependencies on the different characteristics presented in Fig. 1. Results from our numerical study can be compared in a general way with theoretical and numerical results obtained for two-dimensional $\pm J$ Ising lattices. This will allow to bring out the influence that connectivity and dimensionallity have on each of the different properties reported below.

Spins interact via an Ising Hamiltonian of the form

$$H(N) = \sum_{i<j}^{N} J_{ij} S_i S_j \ , \tag{1}$$

where J_{ij} stays for the type of interaction ($+1$ for AF and -1 for F), while S_i is the normal Ising spin orientation degree of

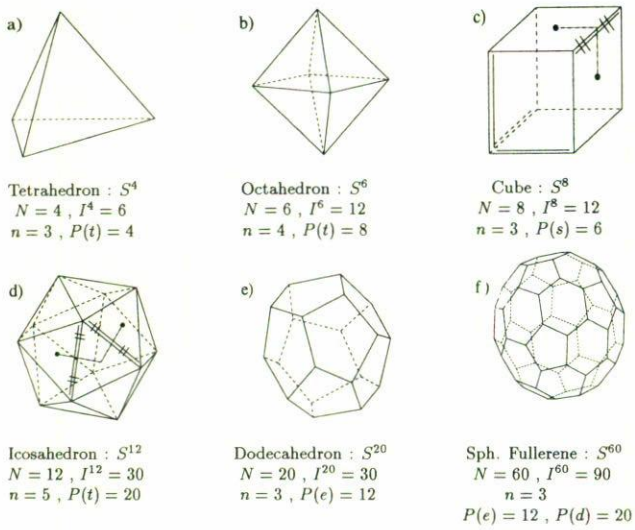

FIGURE 1. Polyhedra considered in this paper and their main characteristics. N: number of spins or "size" of the polyhedron; I^N: number of total interactions; n: coordination number; P: number of plaquettes that can be adapted to explicitly show the kind of plaquette we are refering to $P()$ (t: triangular, s: square, e: pentagonal, d: hexagonal). Single (double) lines at the edges represent F (AF) interactions. Curved plaquettes (marked by dots at the centers) are joined by frustration segments.

freedom ($+1$ or -1 for simplicity). A state corresponds to a set of N ordered spins. Such Hamiltonian is invariant under the inversion of all spins so it is enough to look at the 2^{N-1} independent states. The number of terms in the sum varies when going over the different polyhedra and it is equal to I^N, the number of interactions in each case, when we consider nearest-neighbor interactions only. The ratio between the number of F interactions over I^N is precisely the concentration x. For each possible x in a given system, R randomly prepared samples were fully calculated ($R = 1000$ for the different systems, except S^{60}, where $R = 500$). We have developed computational algorithms for each kind of polyhedron, allowing exact knowledge of all possible ground states and zero-temperature properties of each sample. Self-averaging properties reported below represent average values over the R independent samples.

2. Basic definitions

We will briefly review the definitions of the main properties to be calculated and discussed below. We begin with topological considerations refered to the real lattice to continue with properties based on the ground states.

A *plaquette* is defined as the minimal closed circuit formed by interactions [5]. Thus, plaquettes are equilateral triangles for S^4, S^6, and S^{12}, they are squares for S^8, they are pentagons for S^{20}, while S^{60} presents a mixture of pentagonal and hexagonal plaquettes. A plaquette is said to be frustrated or curved when it is formed by an odd number of AF interactions, so not all these interactions can be simultaneously satisfied when going around the circuit. In Fig. 1 curved plaquettes are marked by dots at the center. The number of curved plaquettes in a given sample will be denoted by P_C.

A topological theorem [6–8] says that the distribution of curved plaquettes determines the thermodynamic properties at 0 K. This is achieved by joining curved plaquettes in pairs by means of imaginary lines going over the centers of these and other intermediate plaquettes; such lines are called *frustration segments*. The length λ of a frustration segment is the number of crossed interactions, that turn out to be frustrated for that ground state. In Fig. 1c we illustrate a frustration segment of length 1 joining two square curved plaquettes. In Fig. 1d we show a frustration segment of length 2 going through a flat plaquette joining two triangular curved plaquettes. All frustration segments that define a ground state add up to the *frustration length of the ground state* Λ_g, which corresponds to the total number of frustrated bonds in any of the ground states. Usually, a frustration length can be obtained in many, say W, different ways, each corresponding to a particular way of drawing the $P_C/2$ frustration segments. If the symmetry of Hamiltonian is invoked we realize that for each set of frustration segments there are two antisymmetric spin sets which points to a total ground state degeneracy of $2W$.

The energy of the ground state E_g^N weights with -1 $(-J)$ each satisfied bond and with $+1$ $(+J)$ each frustrated bond. Namely, $E_g^N = -I^N + 2\Lambda_g^N$. To ease comparison among the different polyhedra, it is convenient to normalize this magnitude dividing by I^N, and to label the result for each polyhedron according to N. That is to say

$$\varepsilon_g^N = \frac{E_g^N}{I^N} = -1 + 2\frac{\Lambda_g^N}{I^N} = -1 + 4\frac{\Lambda_g^N}{nN}, \qquad (2)$$

here n is the coordination number for each particular system.

For a particular sample the ground state is obtained by a combination of frustration segments of different lengths. It is interesting to notice that the composition of frustration segments varies from sample to sample. Here we report the average frustration segment of each system considering all frustration segments over all samples. Namely,

$$\langle \lambda_{F_g}^N \rangle = \frac{2\sum_{\rho=1}^{R} \Lambda_{g\rho}^N}{\sum_{\rho=1}^{R} P_{C\rho}^N}, \qquad (3)$$

where ρ runs over the R samples for that case.

Rather than the degeneracy of the ground manifold it makes more sense to study the remanent entropy σ, which can be expressed as

$$\sigma^N = \frac{\ln W}{N}, \qquad (4)$$

where we neglect additive constants and the constant of Boltzmann k_B is taken as unity if temperatures and energies are both measured in units of J.

The *diluted lattice* is defined by removing all interactions that frustrate in any of the W independent ground states [9]. The interactions that remain in the diluted lattice will be called *bonds* and their number will be denoted as B. Then, the ratio formed by the number of bonds in the diluted lattice to the total number of interactions in the original sample will be defined as h_g, the fractional content of unfrustrated interactions. Namely,

$$h_g^N = \frac{B^N}{I^N}. \tag{5}$$

When all ground states are known, parameter h_g^N can also be calculated by means of

$$h_g^N = \frac{1}{I^N} \sum_{i<j}^{N} \left[\left(\sum_{\alpha}^{W} \frac{|S_i^\alpha S_j^\alpha - J_{ij}|}{2} \right) \textbf{div } W \right], \tag{6}$$

where the first sum runs over the I^N pairs of nearest neighbors ij, the second sum goes over α that represents the W independent ground states. Thus, S_i^α is the spin of site i for the state α. The operator **div** means integer division. Two general properties of h_g^N follow from a careful analysis of this expression: this parameter is restricted to the interval $[0, 1]$ and the value of h_g^N is independent of the ergodic separation done on the system. Actually, the result for h_g^N remains unchanged if the sum over α runs over the $2W$ ground states.

The diluted lattice can also be examined in a microscopic way finding that bonds tend to cluster in a non trivial way, forming *unfrustrated regions* [9]. The size r of a region is the number of connected bonds. It turns out that for each topology there are prefered sizes as it will be reported for the large polyhedra.

In a similar way, we can define p_g^N, the fraction of spins that never flip when scanning the W ground states on one half the configuration space defined by the ergodic separation. Then this parameter is very sensitive to the way ergodicity is broken. We will follow a particular way of breaking ergodicity as depicted below using the following definition for this site-order parameter [4]:

$$p_g^N = \frac{1}{N} \sum_{i}^{N} \left(\left| \sum_{\alpha}^{W} S_i^\alpha \right| \textbf{div } W \right), \tag{7}$$

so p_g^N is restricted to the interval $[0, 1]$.

All of the above properties will be calculated for each polyhedron, calculating many samples for a given x, so a reliable average value is obtained reporting functional dependence of the properties with respect to the relative concentration of interactions.

3. Results and discussion

Discussion will be organized in the same order in which definitions were introduced in previous section. Figures 2, 3, 4, 5 and 9 present average results over all samples ($\langle\ \rangle$) for the different properties as functions of x. Special symbols are used to characterize each polyhedron in all these illustrations. The density of points in each curve is in direct correspondence with I^N, as changes in x occur in steps of $1/I^N$. This is indeed the case for all the polyhedra considered here with the exception of S^{60} for which we have used a coarser interval in the intermediate region where all properties show an approximate constant behavior.

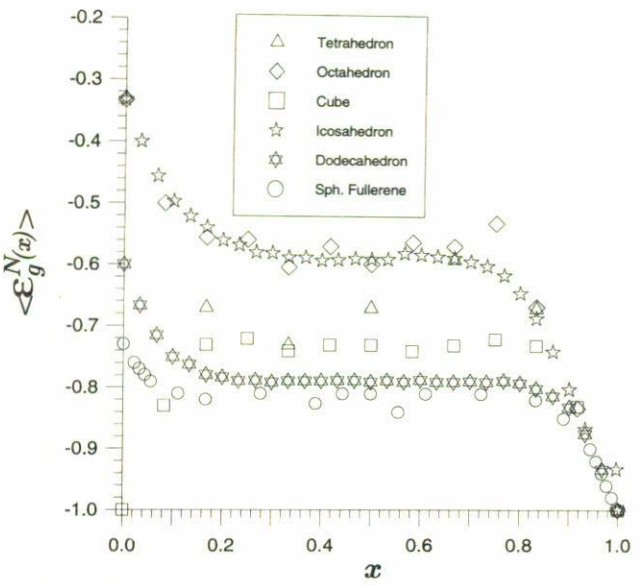

FIGURE 2. Average normalized energies as functions of the concentration of ferromagnetic interactions.

3.1. Energy per interaction $\langle \varepsilon_g^N(x) \rangle$

Average results are presented in Fig. 2. Let us begin the discussion from the limiting values at $x = 0.0$, and $x = 1.0$. For the latter all interactions are F, so no frustration is present, the total energy is $-I^N$, which leads to the trivial ferromagnetic result $\langle \varepsilon_g^N(1.0) \rangle = -1.0$, for all polyhedra. On the other extreme, all interactions are AF that implies that all plaquettes with even number of interactions are flat, while all plaquettes with odd number of interactions are frustrated. Hence, $\langle \varepsilon_g^8(0.0) \rangle = -1.0$. In the case of S^{60} all hexagonal plaquettes are flat while all pentagonal plaquettes are curved joined in pairs by 6 frustration segments all of length 2, leading to $\langle \varepsilon_g^{60}(0.0) \rangle = -66/90 = -0.73$, as can be read in Fig. 2. The remaining polyhedra ($*$) exhibit all their plaquettes curved at $x = 0.0$, with all frustration segments of length unity, leading to the common expression $\langle \varepsilon_g^*(0.0) \rangle = -1.0 + P_C/I^N$. It follows from here that $\langle \varepsilon_g^{20}(0.0) \rangle = -0.60$, and $\langle \varepsilon_g^4(0.0) \rangle = \langle \varepsilon_g^8(0.0) \rangle = \langle \varepsilon_g^{12}(0.0) \rangle = -0.33$. One striking general property is that the average energy per interaction remains constant in the interval $0.2 \leq x \leq 0.8$, with values that reflect a property for each geometry as can be seen in Fig. 2.

The case of equal amount of F and AF interactions, $x = 0.5$, deserves a special discussion because it is at the center of the plateau and it has been a case usually calculated in numerical simulations. In order of increasing energy we find,

$\langle\varepsilon_g^{60}(0.5)\rangle=-0.81$; $\langle\varepsilon_g^{20}(0.5)\rangle=-0.79$; $\langle\varepsilon_g^{8}(0.5)\rangle=-0.73$; $\langle\varepsilon_g^{4}(0.5)\rangle=-0.67$; $\langle\varepsilon_g^{6}(0.5)\rangle=-0.60$; $\langle\varepsilon_g^{12}(0.5)\rangle=-0.59$. We observe that energy is minimized in hexagonal plaquettes, while it is maximized in triangular plaquettes. These results can be compared with simulations in 2 dimensions where $\langle\varepsilon_g(0.5)\rangle=-0.82$, -0.70, and -0.56, for honeycomb, square and triangular lattices respectively [10]. The agreement of the general trend is evident. The case of the dodecahedron, with pentagonal plaquettes, finds no analog in flat two dimensional Bravais lattices. A curiosity is found when comparing S^{12} to S^{20}: although they have the same number of interactions the latter has more energy per bond than the former due to its larger number of plaquettes, therefore many curved plaquettes at $x = 0.5$, thus frustrating more interactions and raising energy.

Systems S^{60} and S^{12} share the value 3 for their coordination number and they have very similar energy per interaction with the spherical Fullerene having a slightly lower value. They have the same number of pentagonal plaquettes, hence the presence of the intrinsic frustration already discussed for the case $x = 0.0$. However, in S^{60} such frustration is diluted by the presence of 20 hexagonal plaquettes; notice that the dilution effect diminishes as x approaches 1.0. Finally, we point out that the cube is the only system to exhibit a symmetric behavior for this parameter. Namely $\langle\varepsilon_g^8(x)\rangle = \langle\varepsilon_g^8(1-x)\rangle$.

3.2. Length of frustration segment $\langle\lambda_g^N(x)\rangle$

Results are presented in Fig. 3, corresponding to averages over all frustration segments found in the sets of R samples for each concentration corresponding to a particular polyhedron. Generally speaking, at $x = 1.0$ no frustration is present and none frustration segment is to be found. As we move to the left, a single AF bond brings in 2 neighboring curved plaquettes leading to frustration segments of length unity for all systems, as it shown at the far right of Fig. 3 for the value $x = (I^N - 1)/I^N$ corresponding to each system. On the other hand, for $x = 0.0$ (all interactions are AF) there are three different situations: *i)* the cube presents no frustration in its square plaquettes and its frustration segment remains undefined; *ii)* S^4, S^6, S^{12}, and S^{20} present fully frustrated plaquettes that can be paired by frustration segments of length unity only, leading to $\langle\lambda_g^N(0.0)\rangle = 1.0$, for $N = 4$, 6, 12 and 20; *iii)* the spherical Fullerene presents 12 pentagonal frustrated plaquettes which do not share any common interaction, since each of them is surrounded by flat hexagonal unfrustrated plaquettes thus leading to frustration segments of length 2.0. All of these values are shown by the numerical simulations presented in Fig. 3.

For intermediate values of x a tendency to constant values in the frustration segment is clearly seen. The case of S^4 is trivial as only frustration segments of length unity are possible; we include this results in Fig. 3 for completeness only. On the other hand, S^{60} drops very quickly from the value 2.0

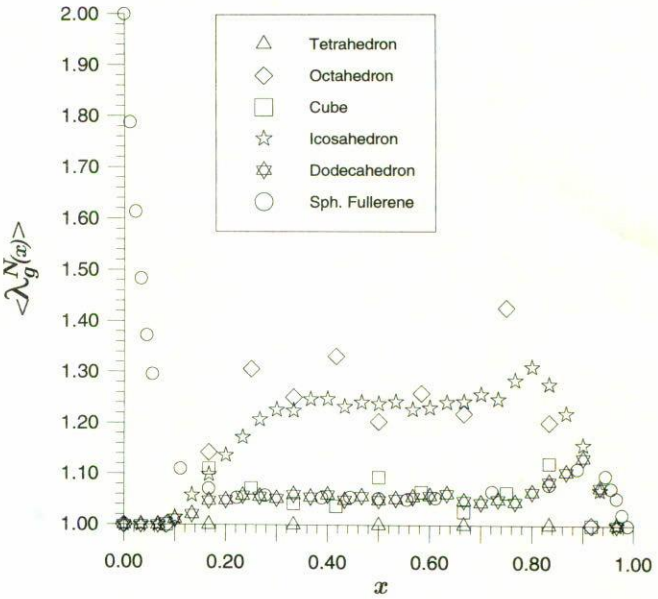

FIGURE 3. Average lengths of frustration segments as functions of the concentration of ferromagnetic interactions.

to a value slightly over 1.0 when as few as 15 AF interactions are present, reaching a value that remains approximately constant from there on. Tendencies segregate in two groups according to the coordination number of the systems. Lower average frustration segments correspond to polyhedra with coordination number 3, namely, for S^8, S^{20}, and S^{60}, while S^6 and S^{12} possess larger values for their average frustration segments. Numerical simulations render the following values at the middle of the range: $\langle\lambda_g^{60}(0.5)\rangle=1.06$; $\langle\lambda_g^{20}(0.5)\rangle=1.05$; $\langle\lambda_g^{8}(0.5)\rangle=1.09$; $\langle\lambda_g^{6}(0.5)\rangle=1.20$; $\langle\lambda_g^{12}(0.5)\rangle=1.24$. It is interesting to notice that $\langle\lambda_g^{60}(0.5)\rangle$, $\langle\lambda_g^{20}(0.5)\rangle$, and $\langle\lambda_g^{8}(0.5)\rangle$ have coordination number 3, as in honeycomb lattices for which it holds that $\langle\lambda_g(0.5)\rangle=1.1$ as obtained by theoretical models [10] and numerical simulations [4] in good agreement with present results. The coordination number is 4 in the case of S^6 as in flat square lattices for which $\langle\lambda_g(0.5)\rangle=1.2$ [10], in perfect agreement with our results. The case of S^{12}, with coordination number 5 admits no direct comparison with Bravais two-dimensional lattices. However, it is interesting to point out that for triangular lattices with coordination number 6 it is found that $\langle\lambda_g(0.5)\rangle=1.3$ [10], which makes the result $\langle\lambda_g^6(0.5)\rangle=1.24$, found here quite on the general tendency. All this discussion allows us to conclude that $\langle\lambda_g^N(x)\rangle$ is primarily determined by the coordination number of the lattice.

3.3. Remanent entropy $\langle\sigma^N(x)\rangle$

Average results are presented in Fig. 4. For x=1, we always get the ferromagnetic singlet which means $\sigma^N(1.0)$=0.0, for all N. At the other extreme, it is only the cube that presents an unfrustrated antiferromagnet, leading also to null remanent entropy. All other cases can be calculated by basic com-

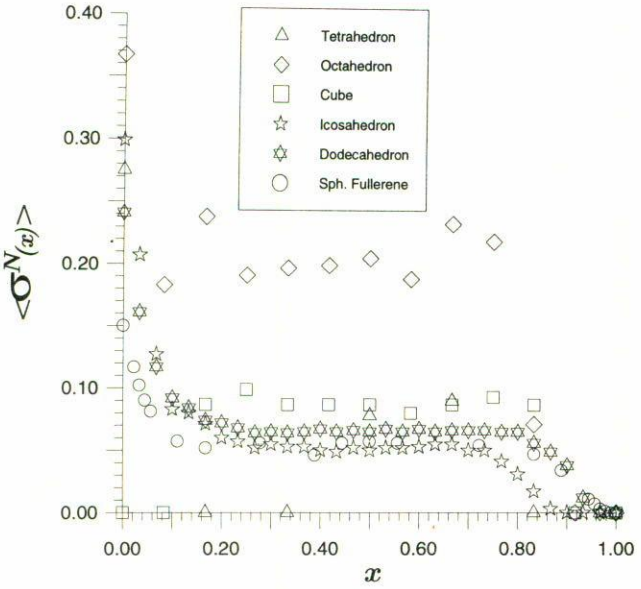

FIGURE 4. Average remanent entropies as functions of the concentration of ferromagnetic interactions.

binatorial analysis. S^4 needs 2 frustration segments to join the two pairs of curved plaquettes, which can be achieved in 3 different ways, therefore $\langle\sigma^4(0)\rangle = (1/4)\ln 3 = 0.275$.

The degeneracy of the octahedron is less obvious. Let us suppose we orientate the octahedron so we can talk about a top triangular plaquette (North), a bottom triangular plaquette (South) and six lateral plaquettes. The top plaquette can be joined by a frustration segment to any of its 3 neighboring lateral plaquettes; so does the bottom plaquette in a completely independent way; the four remaining lateral plaquettes can be joined in two pairs in a unique way. The degeneracy of this system is then given by the product $3 \times 3 \times 1 = 9$, leading to $\langle\sigma^6(0)\rangle = (1/6)\ln 9 = 0.366$.

S^{12} can be solved in a similar manner. Again we have triangular plaquettes at the North and at the South. We also find 18 lateral triangular plaquettes, separated in two groups by an equatorial contour (not on a plane) formed by 6 AF interactions. Both the top and the bottom plaquettes join any of their respective 3 neighboring lateral plaquettes in 3 independent ways. The remaining 8 "northern" lateral plaquettes and the 8 "southern" lateral plaquettes are so packed that they find only 4 different ways in which they can be paired. Therefore the degeneracy is $3 \times 3 \times 4$ and the remanent entropy at this extreme is given by $\langle\sigma^{12}(0)\rangle = (1/12)\ln 36 = 0.299$.

A major change occurs when going to S^{20} since plaquettes are now pentagonal presenting more connectivity as compared to the preceding triangular plaquettes. We can now talk about a pentagonal plaquette at the North and a similar one at the South; an equatorial contour (not on a plane) formed by 10 AF interactions separates the 5 "northern" lateral plaquettes from the 5 "southern" lateral plaquettes. North can pair to any of the "northern" lateral plaquettes in 5 different ways; the same holds for South. The 8 remaining lateral plaquettes can be paired in 5 different ways. The degeneracy is now $5 \times 5 \times 5$ and we get $\langle\sigma^{20}(0)\rangle = (1/20)\ln 125 = 0.241$.

S^{60} can be easily treated due to its similarity with S^{20}. Both present 12 frustrated pentagonal plaquettes when $x = 0$. In both cases they are paired in 125 different ways with frustration segments of length 1 for S^{20} and of length 2 for S^{60}. This makes a huge difference since each of the 6 frustration segments in the spherical Fullerene has two different and independent paths (each going through a different hexagonal plaquette), thus leading to a total degeneracy of 125×2^6. Then, $\langle\sigma^{60}(0)\rangle = (1/60)\ln 8000 = 0.150$.

All of the above theoretical results agree well with the results of the numerical simulations as it is shown at the extreme left in Fig. 4. Again we find a tendency to constant results for the approximate interval $0.2 \leq x \leq 0.8$, except an irregular behavior of S^4 due to its small size and S^6 to a lesser extent. We leave out of this discussion the case of the tetrahedron. At $x = 0.5$ remanent entropies take values between 0.05 and 0.10, excepting the octahedron whose remanent entropy is around 0.20 at the center of the interval. Results for small square and triangular lattices in two dimensions give $\langle\sigma(0.5)\rangle \approx 0.11$ [4], while the tendency in the thermodynamic limit has been estimated at 0.07 [6]. Therefore, the polyhedral lattices present remanent entropies in general agreement with two-dimensional lattices. In a refined analysis we find that the lower entropy is presented by the spherical Fullerene and the icosahedron. On the contrary, the octahedron presents a large entropy, contrasting with the icosahedron that also presents triangular plaquettes. However, in S^6 there is always a double route for all frustration segments of length two thus raising degeneracy, while in S^{12} frustration segments of length two have only one possible path.

The icosahedron falls faster to $\langle\sigma(x)\rangle$=0.0 (a singlet) than any of the other systems so its plateau is also smaller as compared to other polyhedra. As $x \to 1.0$ the number of AF interactions diminishes and they tend to be distributed evenly through the lattice producing pairs of neighboring curved plaquettes that can be joined by frustration segments of length unity uniquely. This is a common feature to all polyhedra under consideration. However, the icosahedron presents the unique property by which all frustration segments of length 2 and 3 occur in only one possible way, while in the other polyhedra they can occur in several possible ways. Then for S^{12} the singlet is reached at x values clearly under 0.9.

3.4. Fractional content of unfrustrated interactions $\langle h_g^N(x)\rangle$

Average results are presented in Fig. 5. In the ferromagnetic limit ($x = 1.0$) no frustration is present in any of the systems and the common result $\langle h_g^N(1.0)\rangle = 1.0$, holds. On the other extreme, at $x = 0.0$, S^8 presents no frustration leading to $\langle h_g^8(0.0)\rangle = 1.0$, for a perfectly ordered AF cube. The cases with pentagonal and triangular plaquettes exclusively (S^{20}, S^4, S^6, and S^{12}) present full frustration and $\langle h_g^*(0.0)\rangle = 0.0$, for them. In the case of S^{60} in the AF limit the 12 pentagonal

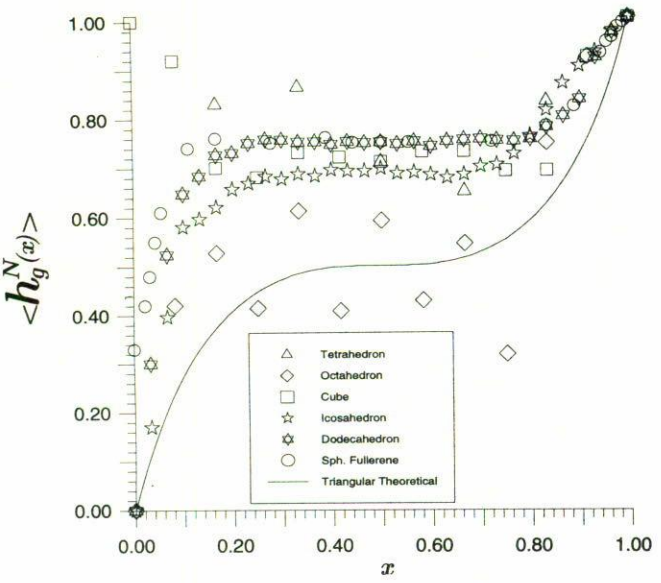

FIGURE 5. Average fractions of unfrustrated interactions as functions of the concentration of ferromagnetic interactions. Solid line represents a theoretical expression valid for flat triangular lattices.

plaquettes are frustrated, while the 20 hexagonal plaquettes remain unfrustrated; then, the 30 interactions between hexagonal plaquettes are the only ones that never frustrate, leading to $\langle h_g^{60}(0.0)\rangle = 30/90 = 0.33$, as corroborated by the numerical simulations of Fig. 5.

In the central portion of Fig. 5 we find again a tendency to constant values except for S^4 and S^6 due to their small sizes. For the case of the latter, a clear modulation is seen: systems with odd number of AF interactions lead to more frustration than the case of even number of AF interactions, which is reflected in the oscillatory results of $\langle h_g^6(x)\rangle$ presented in Fig. 5. Triangular lattices on the plane exhibit a similar general tendency as shown by the continuous curve in Fig. 5. Such a curve was obtained by the method of the sublattice [10] and it is followed closely by results of numerical simulations. Here, it represents the average tendency for $\langle h_g^6(x)\rangle$.

Another system with triangular plaquettes is S^{12} which can be seen to follow the general tendency of the curve obtained for triangular plaquettes on the plane, although the numerical values are higher here. This speaks of less frustration in $\langle h_g^{12}(x)\rangle$ as compared to $\langle h_g^6(x)\rangle$. The reason is the same already discussed above: frustration segments of length 2 occur with two possible trajectories (thus frustrating several different interactions) in S^6, while only one trajectory is possible for segments of length 2 in S^{12}.

The general tendency of the theoretical curve for triangular lattices is even followed by S^{20} formed by pentagonal plaquettes (also odd number of elements). Results are displaced to higher values of the parameter as a consequence of the dominance of frustration segments of length unity between neighboring pentagonal plaquettes, with only one possible trajectory, leading to fewer frustrated interactions than in triangular plaquettes. Results for S^{60} are very close to those of S^{20}, reflecting the similarities between these two systems.

Again, the cube is the only system to exhibit symmetry with respect to x=0.5 due to the invariance of curved plaquettes under an interchange of F and AF interactions. The general tendency here follows the curve for square lattices (not shown) obtained also by the method of the sublattice [10].

At $x = 0.5$ we find that systems with triangular plaquettes show the lower values: $\langle h_g^6(0.5)\rangle = 0.59$, and $\langle h_g^{12}(0.5)\rangle = 0.70$. Then we find the only system with square plaquettes: $\langle h_g^8(0.5)\rangle = 0.71$. The higher values for this parameter are for systems with pentagonal and hexagonal plaquettes: $\langle h_g^{20}(0.5)\rangle \approx \langle h_g^{60}(0.5)\rangle = 0.75$. In two-dimensional systems it is found that $\langle h_g(0.5)\rangle$ takes the value 0.50 for triangular and square lattices, while it is 0.75 for honeycomb lattices. All of this allows concluding that values for $\langle h_g^N(x)\rangle$ are mainly decided by the geometry of the plaquettes.

3.5. Unfrustrated domains in diluted lattices

Unfrustrated interactions or bonds form the diluted lattice of each individual sample. It turns out that bonds tend to cluster in regions free of frustration each behaving as a partial spin glass. Here we study size distributions of such regions for polyhedra with $N \geq 12$. For each system, at a given concentration x, regions of a given size r are counted through the R randomly prepared samples. Results for this spectral analyses will be presented in figures combining different concentrations for the same system.

3.5.1. S^{12}

At $x = 1.0$ there is only one region of size 30, while for $x = 0.0$ the diluted lattice is empty and no regions can be defined. Size distributions for $x_1 = 5/30$, $x_2 = 15/30$, and $x_3 = 25/30$ are presented in Fig. 6. A general comment refers to the presence of the three concentrations through almost the entire range of possible sizes. However, some peculiarities arise for each concentration at certain sizes. Thus, for x_1, at least 10 frustrated plaquettes remain which explains the absence of regions with $r > 25$. At this concentration, domains of small size are preferred due to the prevalence of high frustration. On the other hand, for x_3 regions of larger sizes are the most abundant since frustration is more localized. Regions of size 1 are more abundant for smaller x, in agreement with previous discussion. Regions of size 2 are absent for x_1 and x_3, while they are barely present for x_2, due to topological reasons [11]. A very striking feature is observed for x_3, where several sizes multiples of 5 tend to be preferred to others; this is more evident for sizes such as 5, 10, and 15. Such behavior is a result of the topology of this system where it is possible to draw contours involving 5 bonds in many different ways; on each side of the contour the number of bonds can be a multiple of 5. The distribution for x_2 exhibits large

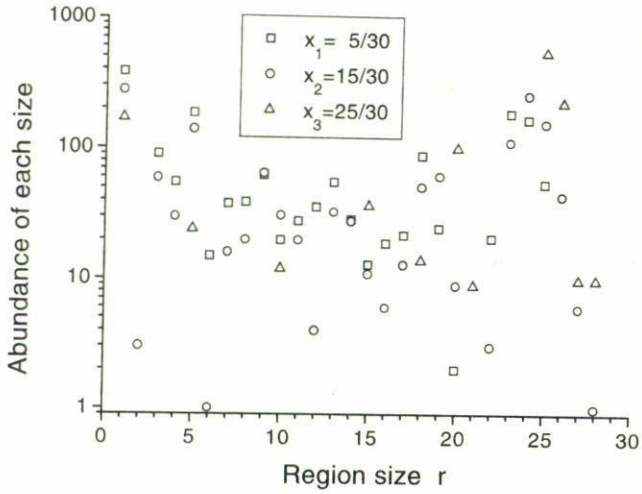

FIGURE 6. S^{12}. Size distribution of unfrustrated regions for three different concentrations of ferromagnetic interactions.

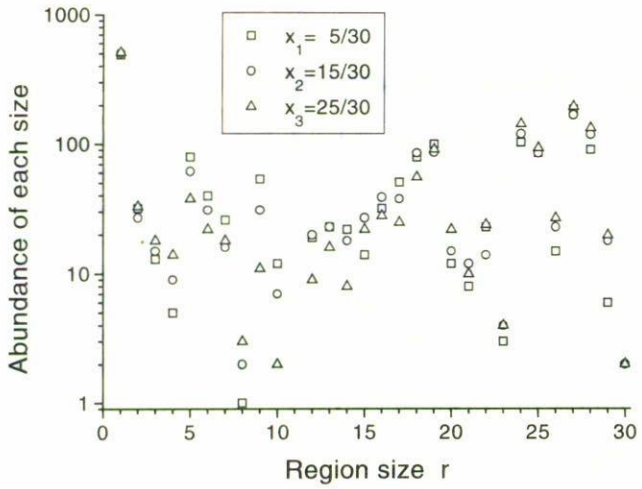

FIGURE 7. S^{20}. Size distribution of unfrustrated regions for three different concentrations of ferromagnetic interactions.

oscillations jumping from a very abundant size ($r = 5$) to an almost nonexistent size ($r = 6$); this is again a manifestation of the topology of these systems which finds preferred sizes and shapes for unfrustrated regions [12].

3.5.2. S^{20}

At $x = 1.0$ there is only one region of size 30, while for $x = 0.0$ the diluted lattice is empty and no regions can be presented in Figs. 6, 7 and 8 can be defined. Size distributions for $x_1 = 5/30$, $x_2 = 15/30$, and $x_3 = 25/30$ are presented in Fig. 7. In spite of having 30 interactions, exactly as S^{12}, results are clearly different from previous case. Differences among concentrations for S^{20} are moderate and they never go beyond one order of magnitude (as it was the case for S^{12}). At small concentrations smaller sizes are preferred. The absence of size $r = 11$ is a common feature for the three concentrations reported here. A region of size 1 is formed when such a bond is common to two flat plaquettes, while

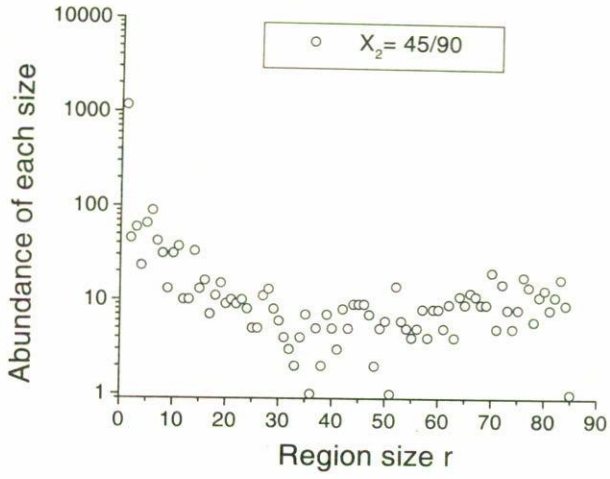

FIGURE 8. S^{60}. Size distribution of unfrustrated regions for equal concentration of ferromagnetic and antiferromagnetic interactions.

the two plaquettes at the ends of the bond must be frustrated. Such a configuration has the same probability for x_1 as for x_3 and approximately the same for x_2 which is verified by the numerical results of Fig. 7.

3.5.3. S^{60}

The extreme cases $x = 1.0$ and $x = 0.0$ allow the same general treatment of two previous cases. We studied several relative concentrations but for simplicity in Fig. 8 we report only the case of equal concentration, namely, $x_2 = 45/90$. All sizes are possible and the distribution shows an approximately flat response for intermediate sizes. For other concentrations a similar picture holds, except at the two extremes. So, for small values of x small regions are the most abundant, while for large values of x large regions tend to dominate.

3.5.4. *General comments*

For the 3 systems recently discussed, the size distribution presents some common features. Abundance of size 1 is an absolute maximum at all concentrations that is a trivial result since necessary conditions for its existence involves fewer plaquettes than for any other size. However, this explanation makes even more striking the absolute maximum presented by S^{12} at $r = 25$ for the largest concentration; a similar but less pronounced situation is exhibited by S^{20} at $r = 27$ for the three concentrations. From a more general point of view we can notice that the three distributions thought as the overlap of two basic broad distributions one centered on a mode at low values of r, and the second one centered at higher values of r.

3.6. Site order parameter $\langle p_g^N(x) \rangle$

Average results are presented in Fig. 9. Before going onto the particular discussions we must remember that numerical cal-

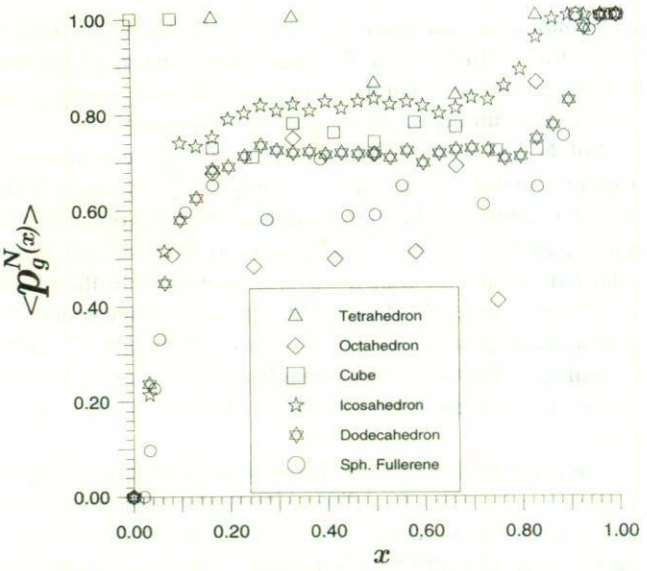

FIGURE 9. Average site order parameters as functions of the concentration of ferromagnetic interactions.

culations for this parameter depend strongly and fundamentally on the way ergodic separation is done. We follow herethe approach of anchoring on the largest unfrustrated domain which is the only region that never overturns. This approach has been justified in general elsewhere [13] so we apply it here to our systems in a direct way.

$\langle p_g^N(x) \rangle$ represents the fraction of spins that do not flip when scanning half the ground states so, at first sight, one may think that it should be directly related to $\langle h_g^N(x) \rangle$. However, this is not so as it can be verified by comparing Figs. 5 and 9. The main reason for the difference is based on the fact that several small regions contribute to $\langle h_g^N(x) \rangle$ without contributing to $\langle p_g^N(x) \rangle$. Small regions can overturn completely, reversing their spins without bringing in frustration. An exception to this behavior is S^6 where these two parameters correlate each other quite well, as discussed below.

At $x = 1.0$, only one unfrustrated domain exists, covering the entire system, leading to $\langle p_g^N(1.0) \rangle = 1.0$ for all systems. On the other hand, at $x = 0.0$, it is only the cube that possesses $\langle p_g^8(0.0) \rangle = 1.0$, due to the lack of frustration. In S^{60} we are left with 30 regions of size 1, so no real large unfrustrated region can be defined leading to $\langle p_g^{60}(x) \rangle = 0.0$. In all other cases we deal with fully frustrated systems in this limit, so the site order parameter $\langle p_g^N(0.0) \rangle$ vanishes for S^4, S^6, S^{12}, and S^{20}.

At intermediate concentrations we have a segregation of results. They have a complex behavior that is not entirely determined by either coordination number or shape of plaquettes. S^4 presents the largest results among all systems. Results for $\langle p_g^4(x) \rangle$ jump from 0.0 (at $x = 0.0$) to 1.0 with just one F interaction going from an empty lattice to another one with a single hole (just one localized frustrated interaction). Such rigid arrangement does not allow any spin flip. On the other hand, S^6, also with triangular plaquettes but a larger coordination number, presents the smallest results for $\langle p_g^6(x) \rangle$ for concentrations defined by odd numbers of F interactions in close relation to results reported in Fig. 5 for $\langle h_g^6(x) \rangle$. System S^{12}, again with triangular plaquettes but with the largest coordination number, shows the second highest results for the site order parameter. The cube presents an intermediate and symmetric behavior. S^{20} gives results just under those obtained for the cube in the intermediate region. Finally, we get S^{60} with a low and slightly oscillatory behavior for $\langle p_g^{60}(x) \rangle$. We can say that $\langle p_g^N(x) \rangle$ is higher in systems where segments of length unity dominate. Oscillations, when they arise, can also be understood in terms of differences of frustration segments by the change of curvature of two neighboring plaquettes by the addition of a single F interaction thus changing the number and length of frustration segments.

At $x = 0.5$ we find the following values 0.86, 0.83, 0.74, 0.71, 0.71, and 0.59, for $\langle p_g^4(0.5) \rangle$, $\langle p_g^{12}(0.5) \rangle$, $\langle p_g^8(0.5) \rangle$, $\langle p_g^{20}(0.5) \rangle$, $\langle p_g^6(0.5) \rangle$, and $\langle p_g^{60}(0.5) \rangle$, respectively.

4. Conclusions

Properties of Ising systems defined on regular polyhedra vary strongly through them according to coordination number, type of plaquette and connectivity among plaquettes for a given frustration length. Superimposed to all this there is a dependence with x, the relative concentration on F interactions.

In the cube all properties are symmetric with respect to $x = 0.5$ since its plaquettes are squares with even number of interactions. In the case of systems with triangular and pentagonal plaquettes (odd number of interactions) there is not symmetry as the system goes from a collection of fully frustrated states at $x = 0.0$ to an unfrustrated ferromagnetic singlet at $x = 1.0$. The case of the spherical Fullerene goes from a partially frustrated situation to the unfrustrated ferromagnetic case.

A common general property shown by all parameters for all systems is that their numerical values tend to be constant (or oscillate around constant values) in the range $0.25 \leq x \leq 0.75$. For some properties and systems this range can be slightly extended to both sides.

Largest values for the energy $\langle \varepsilon_g^N(x) \rangle$ go to higher coordination number. As a second order effect, we find that plaquettes with less sides present higher energy. This is shown in Fig. 2.

For the average frustration segment $\langle \lambda_g^N(x) \rangle$ the general tendency is again that larger values are obtained for larger coordination numbers around $x = 0.5$. No clear second order effects are noticed. Frustration segments elongate toward large values of x before collapsing to $\langle \lambda_g^N(1.0) \rangle = 1.0$. This is a consequence of the increasing probability of having just two curved plaquettes when few AF interactions remain in the system (such pair of plaquettes can be at maximum separation in some samples). This behavior is presented in Fig. 3.

In remanent entropy $\langle \sigma^N(x) \rangle$ it is S^6 the only system that clearly segregates from the rest as seen in Fig. 4. This is due to a unique property of the icosahedron: any frustration segment of length two can be drawn in two possible ways thus increasing the degeneracy for those ground energies. Size N acts as a minor discriminator following the expression (2.3).

The fraction of unfrustrated interactions $\langle h_g^N(x) \rangle$ presents a less trivial behavior. The lowest values are for S^6 for the same reason given in previous paragraph: more possible ways of drawing frustration segments mean a reduced diluted lattice, so $\langle h_g^6(x) \rangle$ presents the lowest values. However, values oscillate according to whether the number of F bonds is odd (lowest values) or even (highest values). The weak dependence is on the number of neighboring plaquettes for each geometry. Thus, for S^{60} each plaquette is surrounded by 6 or 5 plaquettes, so chances are high that a frustration segment of length unity will stay constant frustrating a fixed interaction; this leads to high values for $\langle h_g^{60}(x) \rangle$. A similar situation is obtained for S^{12} with 5 surrounding plaquettes and for S^8 with 4 surrounding plaquettes. This observations can be verified in Fig. 5.

Size of unfrustrated regions presents a bimodal distribution: on one hand there is a tendency to producing many isolated regions of very small size r, while, on the other hand large regions are also highly probable. Regions of intermediate size (around $I/2$) are less likely. Topology strongly modulates this general tendency so some sizes appear as "magic numbers" behaving as almost forbidden for some concentrations. This is clearly seen in Figures 6, 7, and 8, where the logarithmic scale masks the real effect of the two contributions to the bimodal distribution.

Once the criteria of separating ergodically by means of the largest unfrustrated region is used, the site order parameter $\langle p_g^N(x) \rangle$ is the ratio of the number of spins attached to such largest region over the original number of spins in the lattice N. This is a difference with respect to $h_g(x)^N$ where large and small unfrustrated regions contribute. Having established this difference, we conclude that $\langle p_g^N(x) \rangle$ is larger for systems that favor short localized frustration segments, condition that is maximized by S^4 and S^{20}. On the contrary such condition is minimized by S^{60} and S^6. The latter present oscillations with x, since the number of curved plaquettes and the length of frustration segments depend strongly on whether the number of AF interactions is even or odd.

Polyhedral systems relate well to two-dimensional lattices only when the normalized energy $\langle \varepsilon_g^N(x) \rangle$ is considered, where the coordination number establishes the relationship. Then S^4, S^6, and S^{12} stay close to the result for triangular lattices at $x = 0.5$; $S^8(0.5)$ is also close to the result for square lattices; $S^{60}(0.5)$ yields also an average energy in good agreement with honeycomb lattices. Although S^{20} finds no analog in flat two-dimensional Bravais lattices its energy values lay between those for square and hexagonal plaquettes.

For properties other than the normalized energy, no single relationship between two-dimensional and polyhedral systems can be found. Then, beyond a simple geometrical parameter such as coordination number, topology plays an important rôle. Moreover, the effect of topology varies through the different parameters studied here telling that all of them are necessary if Ising spin systems are to be fully characterized.

All of the above conclusions are free from any assumption with respect to boundary conditions. This represents a clear advantage over flat two-dimensional lattices, where some kind of assumption needs to be made to keep the coordination number constant (periodic, antiperiodic or fixed boundary conditions). We have gone over three consecutive values for the coordination number: 3, 4, and 5, which allows us to clarify the rôle of this element separate from dimensionality. In summary, previous conclusions can be read with the idea of stressing the importance of each geometrical and topological element in the properties of closed two-dimensional systems.

Acknowledgments

This work was partially supported by FONDECYT under contract Nr. 199-0878.

1. D. Sherrington and S. Kirkpatrick, *Phys. Rev. Lett.* **35** (1975) 1795.
2. K. Binder and A.P. Young, *Rev. Mod. Phys.* **58** (1986) 801.
3. E.E. Vogel, J. Valdés, and J. Cartes, *Nanostructured Materials* **3** (1993) 441.
4. E.E. Vogel *et al.*, *Phys. Rev. B* **49** (1994) 6018.
5. I. Ono, *J. Phys. Soc. Japan* **41** (1976) 345.
6. J. Vannimenus and G. Toulouse, *J. Phys. C* **10** (1977) 537.
7. G. Toulouse, *Commun. on Phys.* **2** (1977) 115.
8. F. Barahona, R. Maynard, R. Rammal, and J.P. Uhry, *J. Phys. A* **15** (1982) 673.
9. E.E. Vogel *et al.*, *Phys. Rev. B* **58** (1998) 8475.
10. E.E. Vogel and W. Lebrecht, *Z. Phys. B* **102** (1997) 145.
11. W. Lebrecht, M.C. Fuentes, and E.E. Vogel, *Rev. Mex. Fís.* **44** S1 (1998) 85.
12. E.E. Vogel *et al.*, *Physica A* **266** (1999) 425.
13. S. Contreras, M.A. Osorio, and E.E. Vogel, *Rev. Mex. Fís.* **44 S1** (1998) 93.